Hindawi
Journal of Function Spaces
Volume 2022, Article ID 5431057, 15 pages
https://doi.org/10.1155/2022/5431057

Research Article

Collocation Approach Based on an Extended Cubic *B*-Spline for a Second-Order Volterra Partial Integrodifferential Equation

Reny George,[1] **Muhammad Yaseen**,[2] **and Sana Khan**[2]

[1]*Department of Mathematics, College of Science and Humanities in Al-Kharj, Prince Sattam Bin Abdulaziz University, Al-Kharj 11942, Saudi Arabia*
[2]*Department of Mathematics, University of Sargodha, Sargodha, Pakistan*

Correspondence should be addressed to Reny George; renygeorge02@yahoo.com

Received 4 January 2022; Revised 14 March 2022; Accepted 23 March 2022; Published 30 April 2022

Academic Editor: Youssri Hassan Youssri

This paper focuses on an efficient spline-based numerical technique for numerically addressing a second-order Volterra partial integrodifferential equation. The time derivative is discretized using a finite difference scheme, while the space derivative is approximated using the extended cubic *B*-spline basis. The scheme is also tested for stability study to ensure that the errors do not accumulate. The convergence of the proposed scheme is also investigated. The scheme's key benefit is that the approximate solution is produced as a smooth piecewise continuous function allowing us to approximate the solution at any location in the domain. Numerical study is performed, and the comparison of results is made to previously reported results in the literature to show the efficiency of the suggested scheme.

1. Introduction

Integro-Differential Equations (IDEs) are equations that involve both integrals and derivatives of an unknown function. These equations appear very commonly as mathematical models in various fields. Abel, Lotka, Fredholm, Malthus, Verhulst, and Volterra utilized the integral equations and IDEs [1] to study the problems of physics, economics, and mathematical biology. A vast number of research papers and books are devoted to the ongoing phase of the initiative and growth of IDEs over the last few decades. Special implementation of IDEs to deal with statistical models of spatial-temporal development of epidemics was discussed in [2].

Many methods have been used to approximate IDEs previously. The Jacobi-spectral method was used by Ali [3] to approximate the integrodelay differential equations with a weakly singular kernel. Ogunlaran and Oke [4] presented the numerical solution of first order IDEs. Chrysafinos [5] used the method of wavelet-Galerkin to solve IDEs numerically. Abbas et al. [6] approximated IDEs using the direct method of multiwavelet. The first order linear Fredholm IDEs has recently been solved using the rationalized form of Haar functions by Bhrawy et al. [7]. For the numerical solution of Fredholm IDEs, Behiry and Hashish [8] utilized the wavelet technique. The finite element method was used by Chen et al. [9] to approximate the parabolic IDEs. The parabolic Volterra IDEs were approximated by Fakhar and Dehghan [10] using the spectral technique.

In several problems of applied sciences, partial integro-differential equations (PIDEs) are used to represent the complex systems in physical, chemical, and biological sciences and population dynamics [11–19]. Such systems have been solved analytically as well as numerically. Several researchers have contributed to present the numerical solutions of PIDEs using different numerical schemes such as finite differences, Sinc-collocation method, finite element method, spectral collocation method, Legendre method, Galerkin method, and quasiwavelet-based method. Tang [20] approximated PIDEs by using a finite difference scheme. Dehghan [21] gave an approximate solution to a PIDE arising in viscoelasticity. Zarebnia [22] approximated PIDEs by using Sinc-collocation method. Quasiwavelet methods were used by Long et al. [23] to solve PIDEs numerically. Yang et al. [24] used the Crank-Nicolson/quasiwavelet-based numerical

method to approximate a class of PIDEs. Izadi and Dehghan [10] developed spectral methods for parabolic Volterra IDEs. Legendre multiwavelet collocation method was proposed for the numerical solution of PIDEs by Aziz and Khan [25]. Numerical solution of Volterra partial integrodifferential equations based on Sinc-collocation method was presented by Fahim et al. [26]. Izadi and Dehghan [27] developed an effective pseudospectral Legendre-Galerkin technique to solve a nonlinear PIDE emerging in population dynamics. A piecewise polynomial function of degree $n-1$ is a spline function of order n. B-spline-based numerical methods for curves and surfaces were first proposed in the 1940s but were strengthened in the 1970s by various experts. B-splines come in a variety of shapes and sizes, including uniform, nonuniform, rational, and nonrational. Cubic B-spline is a fourth-order B-spline of degree three. The extended cubic B-spline also has a free parameter that allows for local control of this form of B-spline. Collocation techniques based on B-splines proven to be quite effective at approximating the IDEs. Amir and Shakibi [28] used B-spline interpolation to numerically solve IDEs. Exponential splines were used to find the numerical solutions of linear Fredholm IDEs by Tahernezhad and Jalilian [29]. For approximating linear stochastic IDE of fractional order, Mirzaee and Alipour [30] used a cubic B-spline-based collocation method. For a class of hyperbolic PIDE, Fairweather [31] utilized spline-based collocation technique. Gholamian and Saberi-Nadjafi [32] proposed a cubic B-spline collocation technique for a class of PIDEs. Ali et al. [33] developed a quartic B-spline collocation approach for solving PIDEs with a weakly singular kernel. Trigonometric cubic B-spline-based collocation method was used to solve PIDEs by Ali et al. [34].

In this paper, we consider the following second order Volterra PIDE:

$$\frac{\partial v(x,t)}{\partial t} = \int_0^t (t-z)^{-\gamma} \frac{\partial^2 v(x,z)}{\partial x^2} dz + g(x,t), a \le x \le b, t \ge 0, 0 < \gamma < 1, \tag{1}$$

subjected to initial condition,

$$v(x,0) = \varphi(x), \tag{2}$$

and the boundary conditions,

$$\begin{cases} v(a,t) = 0, \\ v(b,t) = 0, \end{cases} t \ge 0, \tag{3}$$

where $a, b, \varphi(x)$, are given and $0 < \gamma < 1$. Motivated by the popularity of the spline approach, we have utilized the extended cubic B-spline to numerically study the above second order Volterra PIDE.

The rest of the paper is organized as follows. In Section 2, extended cubic B-spline-based collocation method is derived in detail. In Sections 3 and 4, the stability and convergence of the proposed scheme are discussed, respectively. Section 4 compares numerical results with some other numerical techniques available in literature. Section 5 summarizes the conclusions of this study.

2. Derivation of the Scheme

Let $\Delta t = t/Q$ denotes the time, and $h = b - a/N$ denotes the space step sizes, with Q and N being positive integers. Set the partitions, $t^q = q\Delta t (0 \le q \le Q)$ and $x_n = nh (0 \le n \le N)$ of both the temporal and spatial domain. The knots x_j evenly discretize the spatial domain $a \le x \le b$, and the interval $[a,b]$ is divided into N subintervals, $[x_j, x_{j+1}]$ of equal length h, $j = 0, 1, 2, \cdots, N-1$, where $a = x_0 < x_1 < \cdots < x_{n-1} < x_N = b$. The numerical solution $V(x,t)$ to the exact solution $v(x,t)$ of (1) is acquired by

$$V(x,t) = \sum_{j=-1}^{N+1} C_j(t) B_j^4(x,\eta). \tag{4}$$

Here, $C_j(t), j = -1, \cdots N+1$ is time-dependent unknowns that must be evaluated and $B_j^4(x,\eta)$ are extended cubic B-spline (ECuBS) basis functions provided by [35].

$$B_j^4(x,\eta) = \frac{1}{24h^4} \begin{cases} 4h(1-\eta)(x-x_j)^3 + 3\eta(x-x_j)^4, & x \in [x_j, x_{j+1}], \\ (4-\eta)h^4 + 12h^3(x-x_{j+1}) + 6h^2(2+\eta)(x-x_{j+1})^2 & \\ -12h(x-x_{j+1})^3 - 3\eta(x-x_{j+1})^4, & x \in [x_{j+1}, x_{j+2}], \\ (4-\eta)h^4 + 12h^3(x_{j+3}-x) + 6h^2(2+\eta)(x_{j+3}-x)^2 & \\ -12h(x_{j+3}-x)^3 - 3\eta(x_{j+1}-x)^4, & x \in [x_{j+2}, x_{j+3}], \\ 4h(1-\eta)(x_{j+4}-x)^3 + 3\eta(x_{j+4}-x)^4, & x \in [x_{j+3}, x_{j+4}], \\ 0, & \text{otherwise}, \end{cases} \tag{5}$$

where $\eta \in [-8, 1]$. Because of the local support characteristic of ECuBS, only $B_{j-1}^4(x,\eta), B_j^4(x,\eta)$ and $B_{j+1}^4(x,\eta)$ are preserved at the grid point x_j. Consequently, the approximation V^q of $v(s,t)$ at q^{th} time level is given as

$$V(x,t^q) = V^q = \sum_{j=-1}^{N+1} C_j^q(t) B_j^4(x,\eta). \tag{6}$$

The unknowns, $C_j^q(t), j = -1, \cdots, N+1$, are found by using collocation conditions on $B_j^4(x,\eta)$ and the given initial and boundary conditions. As a consequence, the approximations V^q and its essential derivatives are obtained as

$$\begin{cases} V^q = \alpha_1 C_{j-1}^q + \alpha_2 C_j^q + \alpha_1 C_{j+1}^q, \\ (V_x)^q = -\beta_1 C_{j-1}^q + \beta_2 C_j^q + \beta_1 C_{j+1}^q, \\ (V_{xx})^q = \lambda_1 C_{j-1}^q + \lambda_2 C_j^q + \lambda_1 C_{j+1}^q, \end{cases} \tag{7}$$

where $\alpha_1 = 4 - \eta/24, \alpha_2 = 8 + \eta/12, \beta_1 = 1/2h, \beta_2 = 0$, $\lambda_1 = 2 + \eta/2h^2$, and $\lambda_2 = -2 + \eta/h^2$.

Table 1: Error comparison for Example 5 when $\Delta t = 10^{-5}$,and $N = 10$.

Q	ECuBS		TCuBS [34]		CuBS [32]	QBCM [33]	QWM [23]
	L_2	L_∞	L_2	L_∞	L_∞	L_∞	L_∞
50	8.40×10^{-8}	1.13×10^{-7}	5.96×10^{-6}	8.93×10^{-6}	1.24×10^{-6}	1.18×10^{-4}	1.58×10^{-3}
150	1.48×10^{-7}	2.00×10^{-7}	3.09×10^{-5}	4.42×10^{-5}	6.34×10^{-6}	6.75×10^{-4}	7.89×10^{-3}
250	1.90×10^{-7}	2.57×10^{-7}	6.65×10^{-5}	9.45×10^{-5}	1.36×10^{-5}	1.40×10^{-3}	1.61×10^{-2}
350	2.18×10^{-7}	2.98×10^{-7}	1.10×10^{-4}	1.56×10^{-4}	2.25×10^{-5}	2.51×10^{-3}	2.53×10^{-2}
450	2.38×10^{-7}	3.26×10^{-7}	1.60×10^{-4}	2.28×10^{-4}	3.28×10^{-5}	3.70×10^{-3}	3.46×10^{-2}

Discretizing the time derivative in (1) by using forward difference scheme, we obtain

$$\frac{\partial v(x,t)}{\partial t} \approx \frac{V^{q+1}(x) - V^q(x)}{\Delta t}. \tag{8}$$

The term on the RHS of (1) can be written as

$$\int_0^t (t-z)^{-\gamma} v_{xx}(x,z)dz + g(x,t) = \int_0^{t_{q+1}} (t_{q+1}-z)^{-\gamma} v_{xx}(x,z)dz + g(x,t_{q+1}). \tag{9}$$

The first expression on the RHS of (9) is time discretized as

$$\begin{aligned}
\int_0^{t_{q+1}} (t_{q+1}-z)^{-\gamma} v_{xx}(x,z)dz &= \int_0^{t_{q+1}} (z)^{-\gamma} v_{xx}(z, t_{q+1}-z)dz, \\
&= \sum_{r=0}^{q} \int_{t_r}^{t_{r+1}} (z)^{-\gamma} v_{xx}(x, t_{q+1}-z)dz, \\
&= \sum_{r=0}^{q} v_{xx}(z, t_{q-r+1}) \int_{t_r}^{t_{r+1}} (z)^{-\gamma} dz, \\
&= \frac{\Delta t^{1-\gamma}}{1-\gamma} \sum_{r=0}^{q} v_{xx}(x, t_{q-r+1}) \left[(r+1)^{1-\gamma} - (r)^{1-\gamma}\right], \\
&= \frac{\Delta t^{1-\gamma}}{1-\gamma} \sum_{r=0}^{q} l_r v_{xx}(x, t_{q-r+1}),
\end{aligned} \tag{10}$$

where $l_r = (r+1)^{1-\gamma} - (r)^{1-\gamma}$. Equation (1) becomes

$$\frac{v^{q+1}(x) - v^q(x)}{\Delta t} = \frac{\Delta t^{1-\gamma}}{1-\gamma} \sum_{r=0}^{q} l_r v_{xx}^{q-r+1}(x) + g(x, t_{q+1}). \tag{11}$$

Let $W = \Delta t^{2-\gamma}/1-\gamma$, so that the last equation becomes

$$v^{q+1}(x) - W l_0 v_{xx}^{q+1}(x) = v^q(x) + W \sum_{r=1}^{q} l_r v_{xx}^{q-r+1}(x) + \Delta t g(x, t_{q+1}). \tag{12}$$

The discretization of the space derivative is performed by (8) so that (12) reduces to

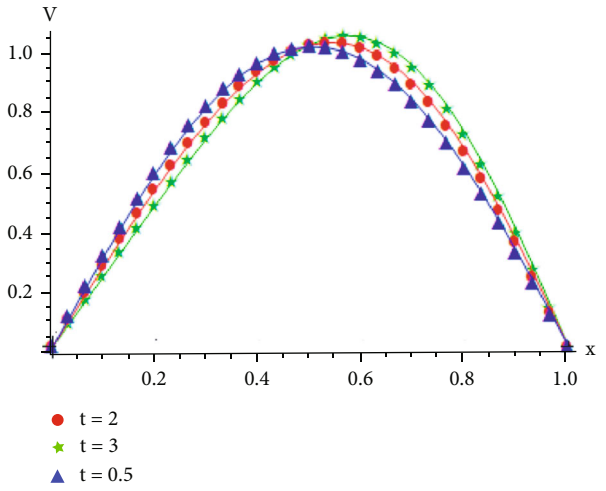

Figure 1: The exact and approximate (triangles, starts, circles) solutions for Example 5 at various times when $h = 0.01$.

$$V^{q+1}(x,\eta) - W V_{xx}^{q+1}(x,\eta) = V^q(x,\eta) + W \sum_{r=1}^{q} l_r V_{xx}^{q-r+1}(x,\eta) + \Delta t g^{q+1}(x). \tag{13}$$

For $x = x_j$, where $j = 0, 1, 2, \cdots, N$, we have

$$V^{q+1}(x_j,\eta) - W V_{xx}^{q+1}(x_j,\eta) = V^q(x_j,\eta) + W \sum_{r=1}^{q} l_r V_{xx}^{q-r+1}(x_j,\eta) + \Delta t g^{q+1}(x_j). \tag{14}$$

Setting

$$G_j = V^q(x_j,\eta) + W \sum_{r=1}^{q} l_r V_{xx}^{q-r+1}(x_j,\eta) + \Delta t g^{q+1}(x_j), \tag{15}$$

we can write, for $j = 0, 1, \cdots, N$,

$$V^{q+1}(x_j,\eta) - W l_0 V_{xx}^{q+1}(x_j,\eta) = G_j \tag{16}$$

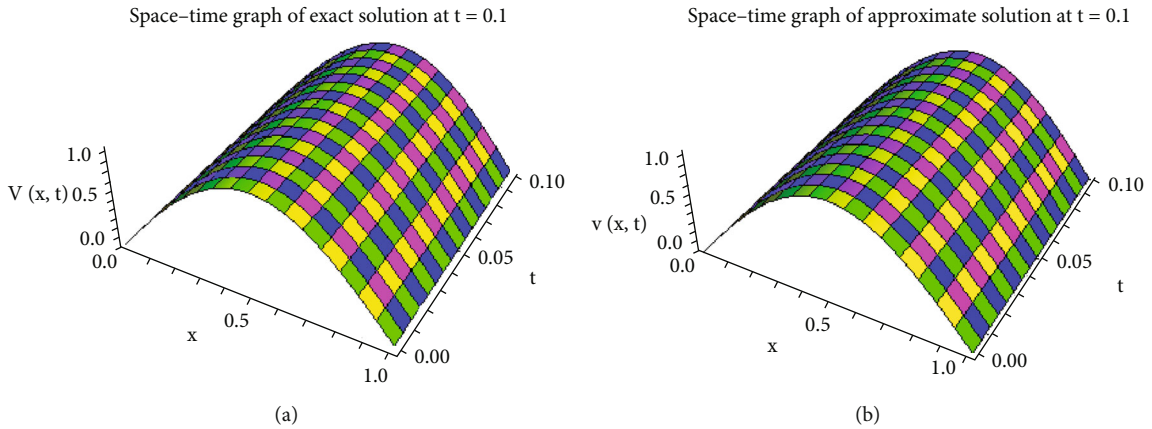

Figure 2: The approximate and exact solutions for Example 5 when $h = 1/60$, $t = 0.1$, $\Delta t = 0.01$.

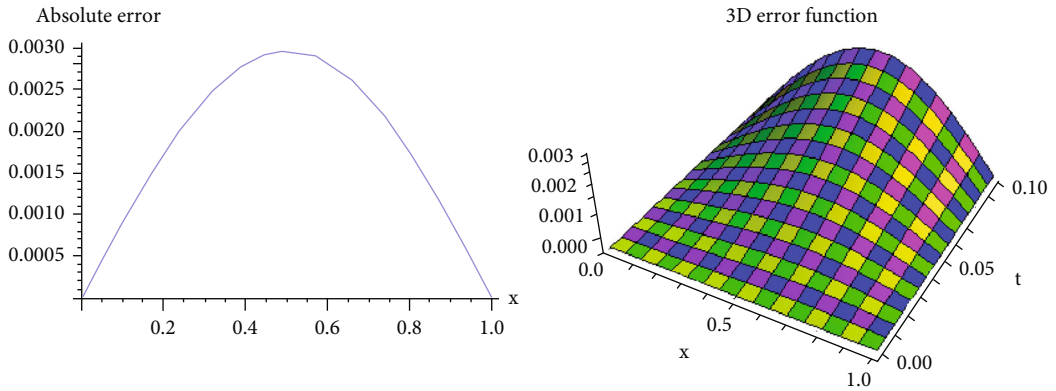

Figure 3: 2D and 3D error profiles for Example 5 when $h = 1/60$, $t = 0.1$, $\Delta t = 0.01$.

This implies that

$$\sum_{j=-1}^{N+1} C_j^{q+1}(t) B_j^4(x_j,\eta) - W \sum_{j=-1}^{N+1} C_j^{q+1}(t) \left(B_j^4\right)''(x_j,\eta) = G_p, \Rightarrow \sum_{j=-1}^{N+1} \left[B_j^4(x_j,\eta) - W\left(B_j^4\right)''(x_j,\eta)\right] C_j^{q+1}(t) = G_j. \tag{17}$$

Equation (17) forms a matrix system of order $(N+1) \times (N+3)$. Approximating the boundary conditions (3) using (7), we obtain two equations from where we remove the unknowns, C_{-1} and C_{N+1}. Consequently, a matrix system of order $(N+1) \times (N+1)$ is generated to acquire the unique solution for this system. The matrix equation for this system is given by

$$SC = G, \tag{18}$$

where the matrices S, C, and G are

$$S = \begin{bmatrix} \omega & 0 & 0 & 0 & \cdots & 0 \\ \rho_1 & \rho_2 & \rho_1 & 0 & \cdots & 0 \\ 0 & \rho_1 & \rho_2 & \rho_1 & \ddots & \vdots \\ \vdots & \ddots & \ddots & \ddots & \ddots & 0 \\ 0 & \cdots & 0 & \rho_1 & \rho_2 & \rho_1 \\ 0 & \cdots & 0 & 0 & 0 & \omega \end{bmatrix}, \tag{19}$$

$$C = \begin{bmatrix} C_0^{q+1} & C_0^{q+1} & \cdots & C_N^{q+1} & C_N^{q+1} \end{bmatrix}^T, \tag{20}$$

$$G = \begin{bmatrix} \vartheta_1(t) & G_0 & G_1 & \cdots & G_N & G_{N+1} & \vartheta_2(t) \end{bmatrix}^T, \tag{21}$$

where $\rho_1 = \alpha_1 - W\lambda_1$ and $\rho_2 = \alpha_2 - W\lambda_2$, $\omega = W\lambda_1/\alpha_1$.

Table 2: Error comparison for Example 6 when $N = 100$,and $\Delta t = 10^{-5}$.

Q	ECuBS		TCuBS [34]		CuBS [32]	
	L_2	L_∞	L_2	L_∞	L_2	L_∞
50	8.37×10^{-10}	1.18×10^{-9}	3.97×10^{-9}	5.61×10^{-9}	6.11×10^{-9}	8.64×10^{-9}
100	5.28×10^{-9}	7.47×10^{-9}	1.41×10^{-8}	1.99×10^{-8}	2.01×10^{-8}	2.84×10^{-8}
150	1.20×10^{-8}	1.71×10^{-8}	2.82×10^{-8}	3.99×10^{-8}	3.93×10^{-8}	5.56×10^{-8}
200	2.08×10^{-8}	2.95×10^{-8}	4.56×10^{-8}	6.45×10^{-8}	6.26×10^{-8}	8.86×10^{-8}
250	3.12×10^{-8}	4.42×10^{-8}	6.59×10^{-8}	9.31×10^{-8}	8.97×10^{-8}	1.27×10^{-8}
300	4.31×10^{-8}	6.10×10^{-8}	8.86×10^{-8}	1.25×10^{-7}	1.20×10^{-7}	1.70×10^{-7}

Initial vector is as follows: the initial condition,

$$v(x_p, 0) = \varphi(x_p), p = 0, 1, 2, 3, \cdots, N \tag{22}$$

can be used to find the initial vector,

$$C^0 = \begin{bmatrix} C_0^0 & C_1^0 & \cdots & C_{N-1}^0 & C_N^0 \end{bmatrix}^T. \tag{23}$$

Equation (22) produces a matrix system of $(N+1) \times (N+1)$ order given as

$$AC^0 = B, \tag{24}$$

where

$$A = \begin{bmatrix} \alpha_1 & \alpha_2 & \alpha_1 & 0 & \cdots & 0 \\ 0 & \alpha_1 & \alpha_2 & \alpha_1 & \cdots & 0 \\ 0 & \ddots & \alpha_1 & \alpha_2 & \alpha_1 & \vdots \\ \vdots & \ddots & \ddots & \ddots & \ddots & \vdots \\ 0 & \cdots & \alpha_1 & \alpha_2 & \alpha_1 & 0 \\ 0 & \cdots & 0 & \alpha_1 & \alpha_2 & \alpha_1 \end{bmatrix},$$
$$C^0 = \begin{bmatrix} c_{-1}^0 & c_0^0 & \cdots & c_N^0 & c_{N+1}^0 \end{bmatrix}^T, \tag{25}$$
$$B = \begin{bmatrix} \varphi(x_0) & \varphi(x_1) & \cdots & \varphi(x_{N-1}) & \varphi(x_N) \end{bmatrix}^T.$$

Once the initial vector C^0 is obtained, the recurrence relation (17) gives the time evolution of vectors C^q, and thus the approximate solution can be calculated.

3. Stability Analysis

In this section, the stability of the proposed method is presented. The proposed scheme is proved stable by using the Von-Neumann stability method. For this purpose, put $g^{q+1}(x) = 0$ in (13) so that

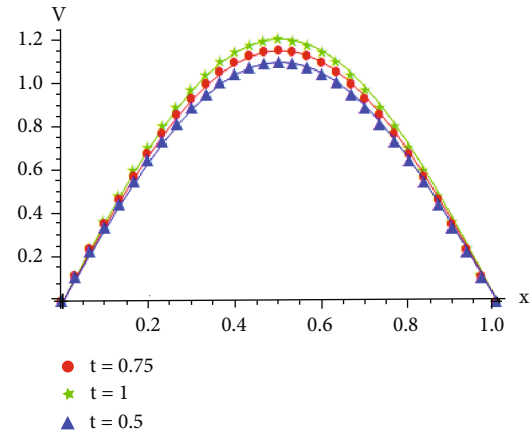

Figure 4: The exact and approximate (triangles, starts, circles) solutions for Example 6 at various times when $h = 0.01$.

$$V^{q+1}(x, \eta) - WV_{xx}^{q+1}(x, \eta) = V^q(x, \eta) + W \sum_{r=1}^{q} l_r V_{xx}^{q-r+1}(x, \eta). \tag{26}$$

Using (8) in (26), we obtain

$$\rho_1 C_{j-1}^{q+1} + \rho_2 C_j^{q+1} + \rho_1 C_{j+1}^{q+1} = \left[\alpha_1 C_{j-1}^q + \alpha_2 C_j^q + \alpha_1 C_{j+1}^q\right] + W \sum_{r=1}^{q} l_r \left[\lambda_1 C_{j-1}^{q-r+1} + \lambda_2 C_j^{q-r+1} + \lambda_1 C_{j+1}^{q-r+1}\right]. \tag{27}$$

Substituting the Fourier mode, $C_j^q = \xi^q e^{\iota j \phi h}$ in (17), where ϕ is the mode number, h is the step size, ξ is the growth factor, $\iota = \sqrt{-1}$, and we obtain

$$K\xi^{q+1} e^{\iota j \phi h} = L\xi^q e^{\iota j \phi h} + \frac{W}{h^2} \sum_{r=1}^{q} M\xi^{q-r+1} e^{\iota j \phi h}, \tag{28}$$

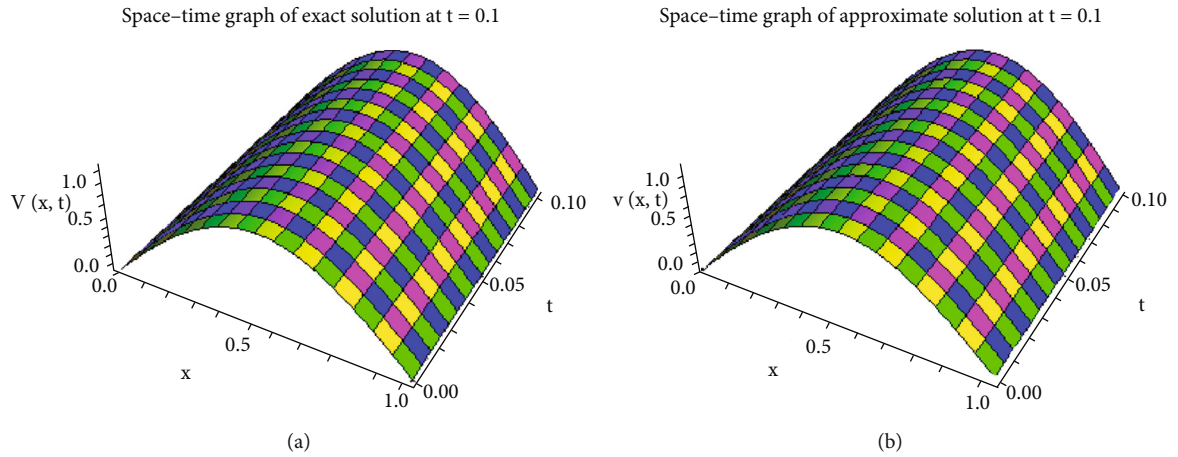

Figure 5: The approximate and exact solutions for Example 6 when $h = 1/60$, $t = 0.1$, $\Delta t = 0.01$.

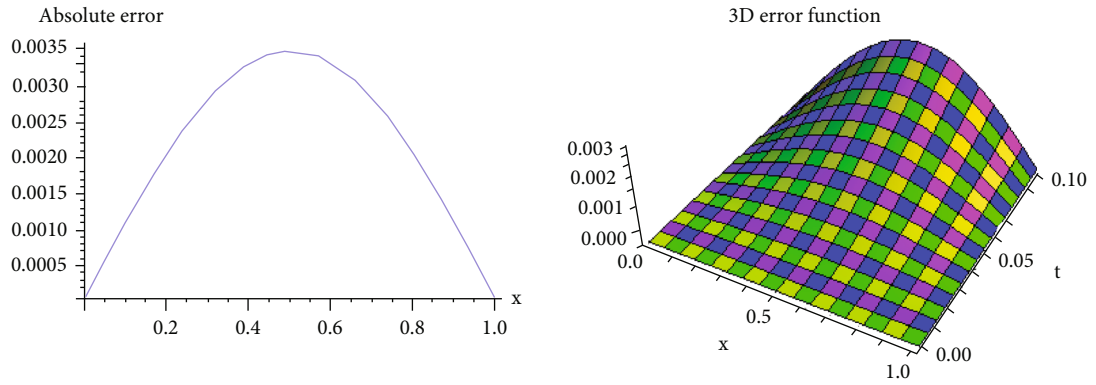

Figure 6: 2D and 3D error profiles for Example 6 when $h = 1/60$, $t = 0.1$, $\Delta t = 0.01$.

where

$$\begin{cases} K = \rho_1\left(e^{-\iota\phi h} + e^{\iota\phi h}\right) + \rho_2, \\ L = \alpha_1\left(e^{-\iota\phi h} + e^{\iota\phi h}\right) + \alpha_2, \\ M = \delta_1\left(e^{-\iota\phi h} + e^{\iota\phi h}\right) + \delta_2, \end{cases} \tag{29}$$

and $\delta_1 = h^2\lambda_1$, $\delta_2 = h^2\lambda_2$. Now, substituting the values of ρ_1, ρ_2, α_1, α_2, δ_1, and δ_2 in (29), we get

$$\begin{cases} K = \left(\dfrac{4-\eta}{24} - W\left(\dfrac{2+\eta}{2h^2}\right)\right)(2\cos\phi h) + \left(\dfrac{8+\eta}{12} - W\left(\dfrac{2+\eta}{h^2}\right)\right), \\ L = \left(\dfrac{4-\eta}{24}\right)(2\cos\phi h) + \left(\dfrac{8+\eta}{12}\right), \\ M = \left(\dfrac{2+\eta}{2}\right)(2\cos\phi h) - (2+\eta). \end{cases} \tag{30}$$

Rearranging the terms of (28) to obtain

$$\xi^q - \left(\frac{L}{K} + \frac{WM}{Kh^2}\right)\xi^{q-1} - \frac{WM}{Kh^2}\sum_{r=2}^{q} l_r\xi^{q-r} = 0. \tag{31}$$

Letting $b_1 = -L/K - WM/Kh^2$ and $b_r = -(WM/Kh^2)l_r$, and $r = 2, \cdots, q$ in (31) to obtain

$$\xi^q + b_1\xi^{q-1} + b_2\xi^{q-2} + \cdots + b_{q-1}\xi + b_q = 0. \tag{32}$$

It is quite clear from (30) that K and L are positive and $M \le 0$. Thus, the coefficients, $b_1, b_2, \cdots b_q$ are positive. Here, it is necessary to mention the following theorem for further procedure.

Theorem 1 (see [36]). *For all roots ξ_j of an arbitrary polynomial $p(\xi) = a_0\xi^n + \cdots + a_n$ with $a_0 \neq 0$, we have $|\xi_j| \le \max\{1, \sum_{j=1}^{n}|a_j/a_0|\}$.*

It is necessary to prove that all the roots, ξ_j, of (32) satisfy $|\xi_j| \le 1$ for stability. Since from Theorem 1, $a_0 = 1$

Table 3: Error comparison for Example 7 when $N = 50$, and $\Delta t = 10^{-4}$.

Q	ECuBS		TCuBS [34]		CuBS [32]	
	L_2	L_∞	L_2	L_∞	L_2	L_∞
50	1.13×10^{-7}	1.73×10^{-7}	2.73×10^{-7}	4.19×10^{-7}	3.48×10^{-7}	5.34×10^{-7}
100	3.49×10^{-7}	5.21×10^{-7}	8.48×10^{-7}	1.26×10^{-6}	1.08×10^{-6}	1.61×10^{-6}
150	6.75×10^{-7}	9.95×10^{-7}	1.64×10^{-6}	2.42×10^{-6}	2.09×10^{-6}	3.08×10^{-6}
200	1.07×10^{-6}	1.57×10^{-6}	2.61×10^{-6}	3.82×10^{-6}	3.33×10^{-6}	4.87×10^{-6}
250	1.54×10^{-6}	2.27×10^{-6}	3.73×10^{-6}	5.51×10^{-6}	4.76×10^{-6}	7.02×10^{-6}
300	2.05×10^{-6}	3.02×10^{-6}	4.99×10^{-6}	7.33×10^{-6}	6.36×10^{-6}	9.35×10^{-6}

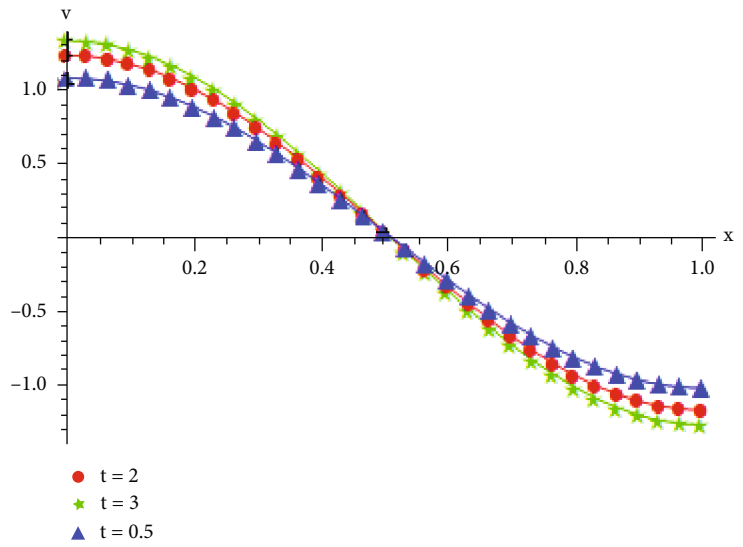

Figure 7: The exact and approximate (triangles, starts, circles) solutions for Example 7 at various times when $h = 0.01$.

and $a_j > 0$, $j = 1, \cdots, q$, we have

$$\sum_{j=1}^{q}\left|\frac{a_j}{a_0}\right| = \left|\frac{-\left(L + \left(WM/h^2\right)\sum_{r=1}^{q} l_r\right)}{K}\right|, \tag{33}$$

where

$\sum_{r=1}^{q} l_r = \sum_{r=1}^{q}[(r+1)^{1-\gamma} - (r)^{1-\gamma}] = (q+1)^{1-\gamma} - 1.()$

Let us assume that $D_\gamma = (q+1)^{1-\gamma} - 1$, then (33) becomes

$$\sum_{j=1}^{q} a_j = \left|-\frac{L + \left(WMD_\gamma/h^2\right)}{K}\right|. \tag{34}$$

From the definition of M in (29), if we let $M = 0$, then $h = 0$. Consequently, (31) becomes

$$\xi^q - \frac{L}{K}\xi^{q-1} = 0 \Rightarrow \xi = 0 \text{ or } \xi = 1. \tag{35}$$

Thus, the required condition for stability is fulfilled that is $|\xi_j| \le 1$. Next, if $\neq 0 (M < 0)$, then from (34), we have

$$-L - \frac{\mathrm{WMD}_\gamma}{h^2} < K, \tag{36}$$

so that the stability condition, i.e., $(|\xi_j| \le 1)$ is satisfied. Now, using the values of K, L, and M in above inequality,

$$-(4-\eta)\cos\eta h - (8+\eta) + \frac{6(2+\eta)}{h^2} W\left(D_\gamma - 1\right)(1 - \cos\eta h) < ,0.$$

$$\cos\eta h > \frac{-(8+\eta/6) + \left((2+\eta)W\left(D_\gamma - 1\right)/h^2\right)}{(4-\eta/6) + \left((2+\eta)W\left(D_\gamma - 1\right)/h^2\right)}. \tag{37}$$

This inequality implies the unconditional stability of introduced scheme.

4. Convergence Analysis

The suggested scheme's convergence analysis for spatial and temporal directions is provided separately in this section.

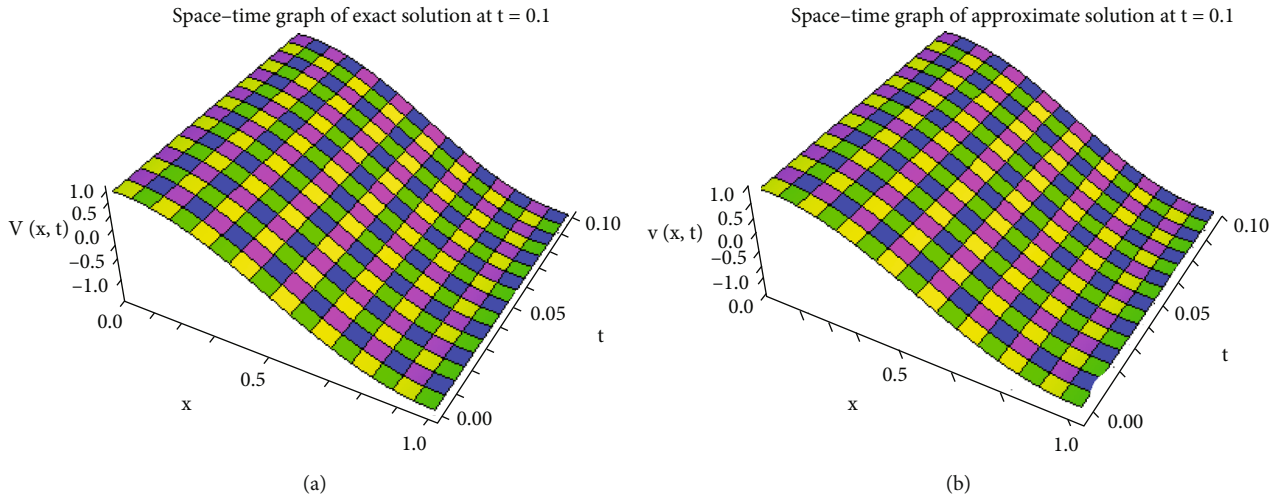

FIGURE 8: The approximate and exact solutions for Example 7 when $h = 1/60$, $t = 0.1$, $\Delta t = 0.01$.

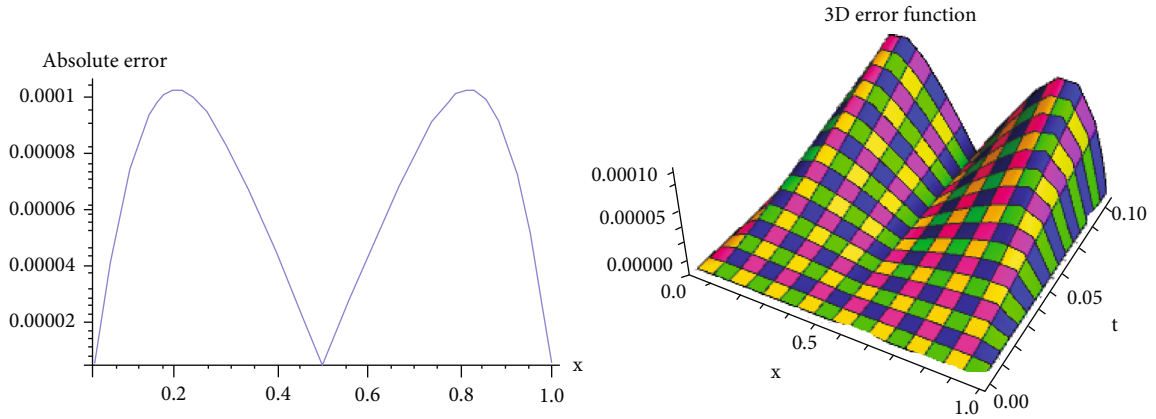

FIGURE 9: 2D and 3D error profiles for Example 7 when $h = 1/60$, $t = 0.1$, $\Delta t = 0.01$.

The convergence is evaluated independently for spatial and temporal directions for this purpose. The following theorem must be proven for spatial convergence.

Theorem 2. *If $\hat{v}(x)$ is the exact solution of equations (1)–(3) and $\hat{b}(x)$ is the B-spline collocation approximation to $\hat{v}(x)$, the technique is then second order convergent, and*

$$\|\hat{v}(x) - \hat{b}(x)\|_{\infty} \leq \sigma h^2, \tag{38}$$

where $\sigma = \kappa_0 Łh^2 + R$ is a finite constant.

Proof. Assume that $\hat{v}(x)$ is the exact solution of equations (1)–(3), then the approximation, $\hat{b}(x)$ to $\hat{v}(x)$, is given by

$$\hat{b}(x) = \sum_{j=-1}^{N+1} \hat{C}_j(t) B_j^4(x, \eta), \tag{39}$$

where $\hat{C} = (\hat{C}_{-1}, \hat{C}_0, \cdots, \hat{C}_{N+1})$. Further, suppose that $\tilde{b}(x)$ is the evaluated extended cubic B-spline collocation approximation to $\hat{b}(x)$, namely,

$$\tilde{b}(x) = \sum_{j=-1}^{N+1} \tilde{C}_j(t) B_j^4(x, \eta), \tag{40}$$

where $\tilde{C} = (\tilde{C}_{-1}, \tilde{C}_0, \cdots, \tilde{C}_{N+1})$. To approximate the error, $\|\hat{v}(x) - \hat{b}(x)\|_{\infty}$, we have to determine the errors, $\|\hat{v}(x) - \tilde{b}(x)\|_{\infty}$ and $\|\tilde{b}(x) - \hat{b}(x)\|_{\infty}$ separately. To compute $\tilde{b}(x)$ and $\hat{b}(x)$, the values of vectors $\hat{C}$ and $\tilde{C}$ must be computed from two linear equations,

$$S\hat{C} = \hat{G}, \tag{41}$$

$$S\tilde{C} = \tilde{G}. \tag{42}$$

Table 4: Error comparison for Example 8 when $\gamma = 1/4$, $N = 50$, and $\Delta t = 10^{-4}$.

Q	ECuBS		TCuBS [24]		CuBS [22]	
	L_2	L_∞	L_2	L_∞	L_2	L_∞
50	1.48×10^{-6}	2.88×10^{-6}	2.29×10^{-6}	4.26×10^{-6}	2.46×10^{-6}	4.53×10^{-6}
100	5.15×10^{-6}	8.37×10^{-6}	7.89×10^{-6}	1.24×10^{-5}	8.44×10^{-6}	1.32×10^{-5}
150	1.06×10^{-5}	1.69×10^{-5}	1.61×10^{-5}	2.50×10^{-5}	1.72×10^{-5}	2.67×10^{-5}
200	1.75×10^{-5}	2.66×10^{-5}	2.66×10^{-5}	3.94×10^{-5}	2.84×10^{-5}	4.19×10^{-5}
250	2.58×10^{-5}	3.89×10^{-5}	3.90×10^{-5}	5.74×10^{-5}	4.17×10^{-5}	6.12×10^{-5}
300	3.53×10^{-5}	5.19×10^{-5}	5.33×10^{-5}	7.76×10^{-5}	5.69×10^{-5}	8.29×10^{-5}

Now, by subtracting (42) from (41), we obtain

$$S\left(\tilde{C} - \hat{C}\right) = \tilde{G} - \hat{G}. \tag{43}$$

The specification of matrix S in equation (19) makes S strictly diagonally dominant making it nonsingular. Thus,

$$\left(\tilde{C} - \hat{C}\right) = S^{-1}\left(\tilde{G} - \hat{G}\right). \tag{44}$$

Taking infinity norm of above equation, we obtain

$$\left\|\left(\tilde{C} - \hat{C}\right)\right\|_\infty \leq \|S^{-1}\|_\infty \left\|\left(\tilde{G} - \hat{G}\right)\right\|_\infty. \tag{45}$$

Let the sum of ith row of matrix $S = [x_{ij}]_{(N+1)\times(N+1)}$ be $\tau_i (0 \leq i \leq N)$. Then, we have

$$\begin{aligned} \tau_0 &= \sum_{j=0}^{N} a_{0j} = \omega, \\ \tau_i &= \sum_{j=0}^{N} a_{ij} = \rho_2 + 2\rho_1 \; i = 1, \cdots, N-1, \\ \tau_N &= \sum_{j=0}^{N} a_{Nj} = \omega. \end{aligned} \tag{46}$$

It is well known in the theory of matrices that

$$\sum_{j=0}^{N} x_{ij}^{-1} \tau_j = 1, i = 0, 1, \cdots, N. \tag{47}$$

Here, x_{ij}^{-1} represents the entries of S^{-1}. Then,

$$\|S^{-1}\|_\infty = \sum_{j=0}^{N} \left|x_{ij}^{-1}\right| \leq \frac{1}{\tau}, \tag{48}$$

where $\tau = \min_{0\leq i\leq N} \tau_i = \min(\omega, \rho_2 + 2\rho_1) = \min(W(2 + \eta/2 h^2)(24/4 - \eta), 1)$. Using (48) in (45) to acquire

$$\left\|\left(\tilde{C} - \hat{C}\right)\right\|_\infty \leq \frac{1}{\tau}\left\|\left(\tilde{G} - \hat{G}\right)\right\|_\infty. \tag{49}$$

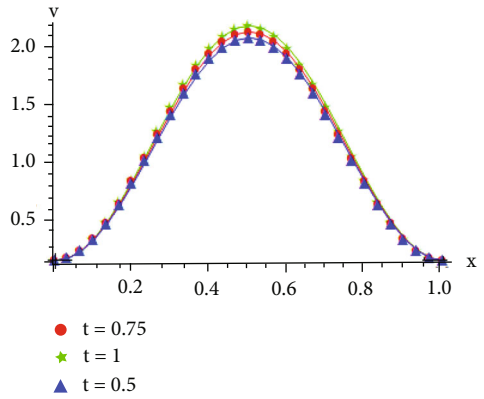

Figure 10: The exact and approximate (triangles, starts, circles) solutions for Example 8 at various times when $h = 0.01$.

Using (15), the upper bound of $\|(\tilde{G} - \hat{G})\|_\infty$ is computed as

$$\begin{aligned} \left|\tilde{G}_i - \hat{G}_i\right| \leq |\tilde{v}_i - \hat{v}_i| + \Delta t\left|\tilde{g}_i^{q+1} - \tilde{g}_i^{q+1}\right| + \frac{W}{h^2}\sum_{r=1}^{q}|l_r| \\ \left(\delta_1\left|\tilde{C}_{j-1}^{q-r+1} - \hat{C}_{j-1}^{q-r+1}\right| + \delta_2\left|\tilde{C}_j^{q-r+1} - \hat{C}_j^{q-r+1}\right| + \delta_1\left|\tilde{C}_{j+1}^{q-r+1} - \hat{C}_{j+1}^{q-r+1}\right|\right). \end{aligned} \tag{50}$$

To simplify the RHS of (50), we present the following theorem. □

Theorem 3 (see [37, 38]). *If $P(x) \in c^4[a, b]$, $|P^4(x)| \leq Ł, \forall s \in [a, b]$, the interval $[a, b]$ is partitioned by $\Delta = \{a = x_0 < x_1 < \cdots < x_N = b\}$ into subintervals of length h. If $b(x)$ is the unique spline function interpolates $P(x)$ at knots $x_0, x_1, \cdots, x_N$, then there exists a constant κ_j such that,*

$$\|P^{(l)} - b^{(l)}\| \leq \kappa_l Ł h^{4-l} l = 0, 1, 2, 3. \tag{51}$$

Using the aforementioned theorem,

$$|\tilde{v}_i - \hat{v}_i| = \left|\tilde{b}_i(x) - \hat{b}_i(x)\right| \leq \kappa_0 Ł h^4. \tag{52}$$

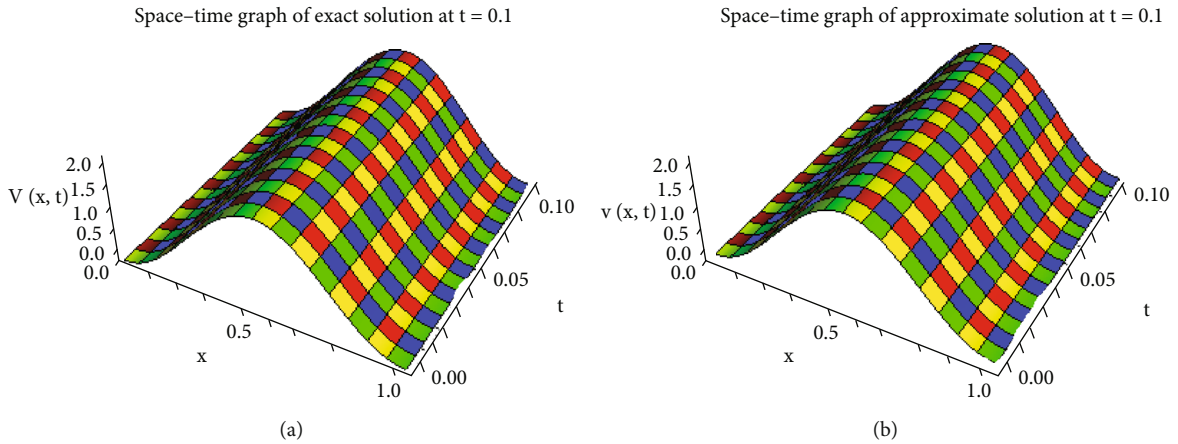

Figure 11: The approximate and exact solutions for Example 8 when $h = 1/60$, $t = 0.1$, $\Delta t = 0.01$.

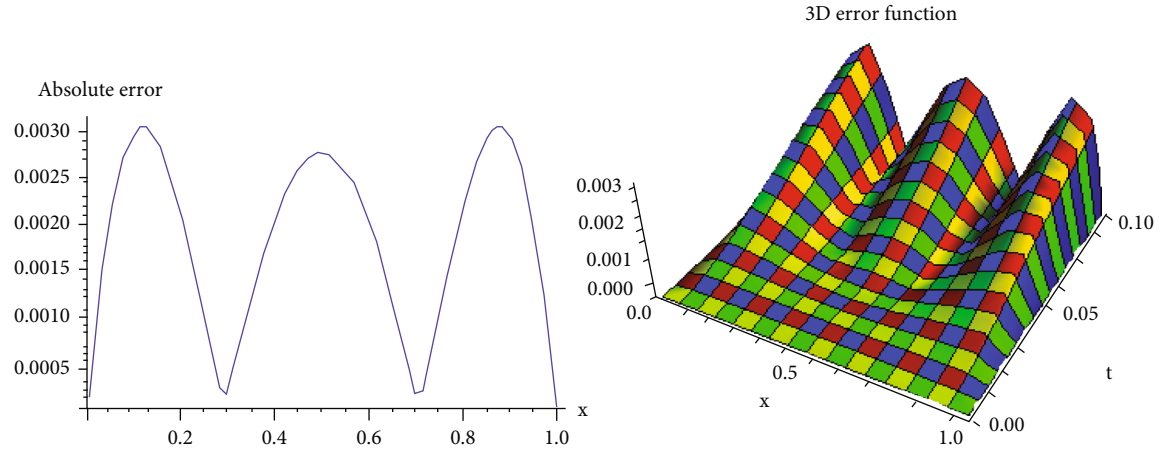

Figure 12: 2D and 3D error profiles for Example 8 when $h = 1/60$, $t = 0.1$, $\Delta t = 0.01$.

Furthermore, $\{l_r\}_{r=1}^{q}$ is a decreasing sequence of positive terms and $l_r \le 1$ for $1 \le r \le n$. Using (52) and letting $\tilde{g}_i^{q+1} = \hat{g}_i^{q+1}$, we can thus write (50) as

$$\left|\tilde{G}_i - \hat{G}_i\right| \le \kappa_0 Łh^4 + \frac{W}{h^2}\sum_{r=1}^{q} d_r. \tag{53}$$

where

$$\left(\delta_1\left|\tilde{C}_{i-1}^{q-r+1} - \hat{C}_{i-1}^{q-r+1}\right| + \delta_2\left|\tilde{C}_i^{q-r+1} - \hat{C}_i^{q-r+1}\right| + \delta_1\left|\tilde{C}_{i+1}^{q-r+1} - \hat{C}_{i+1}^{q-r+1}\right|\right) = d_r. \tag{54}$$

Let $\sum_{r=1}^{q} d_r = D_q$ and $\kappa_0 Łh^4 + (W/h^2)D_q = R_q$, then, (53) becomes

$$\left|\tilde{G}_i - \hat{G}_i\right| \le R_q. \tag{55}$$

Using (55) in (49) to get

$$\left\|\left(\tilde{C} - \hat{C}\right)\right\|_\infty \le \frac{1}{\tau}R_q = Rh^2, \tag{56}$$

where $Rh^2 = (1/\tau)R_q = \max\left((1/W)(2h^2/2 + \eta)(4 - \eta/24), 1\right)$.

To proceed further, we have to follow the next theorem.

Theorem 4 (see [39]). *The B-splines $\{B_{-1}, B_0, B_1, \cdots, B_{N-1}, B_N, B_{N+1}\}$ satisfy the following inequality*

$$\left|\sum_{i=-1}^{N+1} B_i(x)\right| \le 1, 0 \le s \le 1. \tag{57}$$

Now, by subtracting (40) from (39), we have

$$\tilde{b}(x) - \hat{b}(x) = \sum_{j=-1}^{N+1}\left(\tilde{C}_j - \hat{C}_j\right)B_j^4(x). \tag{58}$$

Taking the infinity norm on both sides, we obtain

$$\begin{aligned}\|\tilde{b}(x)-\hat{b}(x)\|_\infty &= \|\sum_{j=-1}^{N+1}\left(\tilde{C}_j-\hat{C}_j\right)B_j^4(x)\|_\infty,\\ &\le \left|\sum_{j=-1}^{N+1}B_j^4(x)\right|\|\left(\tilde{C}_j-\hat{C}_j\right)B_j^4(x)\|_\infty, \le Rh^2,\end{aligned} \tag{59}$$

that is,

$$\|\tilde{b}(x)-\hat{b}(x)\|_\infty \le Rh^2. \tag{60}$$

From Theorem (3) and equation (52), we have

$$\|\hat{v}(x)-\tilde{b}(x)\|_\infty \le \kappa_0 Łh^4. \tag{61}$$

Thus, from (60) and (61), we have

$$\|\hat{v}(x)-\hat{b}(x)\|_\infty \le \|\hat{v}(x)-\tilde{b}(x)\|_\infty+\|\tilde{b}(x)-\hat{b}(x)\|_\infty, \le \kappa_0 Łh^4 + Rh^2 = \sigma h^2, \tag{62}$$

where $\sigma = \kappa_0 Łh^2 + R$.

Now, for temporal convergence, applying Taylor expansion on (16), we have

$$\begin{aligned}&\left(v^q(x)+\Delta t v_t^q(x)+\frac{\Delta t^2}{2}v_{tt}^q(x)+\cdots\right)-T\left(v_{xx}^q(x)+\Delta t v_{xxt}^q(x)+\Delta t v_{xxt}^q(x)+\frac{\Delta t^2}{2!}v_{xxtt}^q(x)+\cdots\right)\\ &\quad = v^q(x)+W\sum_{r=1}^{q}l_r v_{xx}^{q-r+1}(x)+\Delta\left(g^q(x)+\Delta g_t^q(x)\right).\end{aligned} \tag{63}$$

Rearranging terms in above equation, we obtain

$$\begin{aligned}&\Delta t\left(v_t^q-g^q\right)-W\left(l_0 v_{xx}^q+\sum_{r=1}^{q}l_r v_{xx}^{q-r+1}\right)+\Delta v_{xxt}^q\\ &\quad+\frac{\Delta t^2}{2!}v_{xxtt}^q+\frac{\Delta t^2}{2!}\left(v_{xx}^q+g_t^q\right)=O(\Delta t).\end{aligned} \tag{64}$$

Assuming $v(x,t)$ to be the exact and $v^q(x,t)$ the approximate solutions of the equations (1)-(3), we have from (62) and (64) that

$$\|v(x,t)-v^q(x,t)\| \le \rho\left(k+h^2\right), \tag{65}$$

where ρ is a finite constant.

5. Numerical Results

The efficiency and the validity of the suggested methodology are confirmed in this part using various test problems by utilizing the L_2 and L_∞ error norms defined as

$$\begin{aligned}L_2 &= \|V-V_q\|_2 = h\sum_{j=0}^{N}\left|\left(V\left(x_j,t_q\right)-V_j^q\right)^2\right|,\\ L_\infty &= \|V-V_q\|_\infty = \max_j\left|V\left(x_j,t_q\right)-V_j^q\right|.\end{aligned} \tag{66}$$

All numerical calculations have been performed using Mathematica 12.

Example 5 (see [23]). Consider equation (1) with

$$g(x,t)=\frac{2t^{1/2}}{\sqrt{\pi}}\left(\pi^{\frac{5}{2}}\sin(\pi x)-\frac{4t^{3/2}}{\sqrt{\pi}}\sin(2\pi x)\right)-2\pi^{\frac{5}{2}}t^2\sin(2\pi x), \tag{67}$$

subject to the BCs,

$$v(0,t)=v(1,t)=0, 0\le t<1, \tag{68}$$

and the IC,

$$v(x,0)=\sin(\pi x), x\in[0,1]. \tag{69}$$

The analytical solution for this problem is $v(x,t)=\sin(\pi x)-(4t^{5/2}/\sqrt{\pi})\sin(2\pi x)$ with $\gamma=1/2$. The suggested approach is implemented on the aforementioned problem to get numerical results. The estimated errors are compared to those provided in [23, 32–34] at various time stages in Table 1. Figure 1 presents an efficient comparison of approximate and exact solutions at various time levels. 3D comparison between approximate and exact solution is depicted in Figure 2. Figure 3 exhibits the 2D and 3D error profiles. The comparison reveals that the proposed algorithm has far better accuracy. The numerical solution when $h=0.05$, $t=1$, and $\Delta t=0.01$ is given as

$$V(x,1)=\begin{cases}1.43183\times10^{-18}-1.53174x+2.05977\times10^{-14}x^2+\\ 25.8542x^3-6.29505x^4, & x\in\left[0,\frac{1}{20}\right),\\ -0.0000243493-1.52879x-0.118318x^2+27.831x^3-\\ 18.1748x^4, & x\in\left[\frac{1}{20},\frac{1}{10}\right),\\ -0.000218991-1.51313x-0.471333x^2+30.9718x^3-\\ 27.9956x^4, & x\in\left[\frac{1}{10},\frac{3}{20}\right),\\ \vdots & \\ \vdots & \\ 2.92425-32.3551x+104.229x^2-115.32x^3+40.5233x^4, & x\in\left[\frac{17}{20},\frac{9}{10}\right),\\ -6.19315+8.75716x+34.725x^2-63.1058^3+25.817x^4, & x\in\left[\frac{9}{10},\frac{19}{20}\right),\\ -19.686+65.9016x-56.0282x^2+0.949023x^3+8.86352x^4, & x\in\left[\frac{19}{20},1\right).\end{cases}\tag{70}$$

Example 6 (see [32]). Consider the equation (1) with $v(x,t)=(t+1)^2\sin\pi s$ subject to initial and boundary conditions $v(s,0)=\sin\pi s$, $v(0,t)=v(1,t)=0$, respectively. $g(x,t)$ is to be chosen with $\gamma=0.5$.

The suggested technique is applied on the above problem to acquire approximate solutions and absolute errors. Table 2 reports the contrast between the computed errors of present scheme and those of [32, 34] for different time levels. For various time stages, a sharp contrast between exact and approximate solutions is presented in Figure 4. Figure 5 depicts a 3D comparison between exact and approximate solutions. 2D and 3D absolute errors are plotted in Figure 6. The numerical solution when $h=0.05$, $t=1$, and $\Delta t=0.01$ is given as

$$V(x,1)=\begin{cases}7.69735\times10^{-18}+12.4842x+3.76073\times10^{-13}x^2-20.4956x^3+\\ 0.0307403x^4, & x\in\left[0,\frac{1}{20}\right),\\ -0.0000611671+12.4879x-0.0729451x^2-20.0154x^3+\\ 0.091464x^4, & x\in\left[\frac{1}{20},\frac{1}{10}\right),\\ -0.00102794+12.5168x-0.361224x^2-19.0661x^3+\\ 0.149936x^4, & x\in\left[\frac{1}{10},\frac{3}{20}\right),\\ \vdots & \\ \vdots & \\ -6.76161+44.8042x-56.66x^2+18.4664x^3+0.149936x^4, & x\in\left[\frac{17}{20},\frac{9}{10}\right),\\ -7.50901+47.3382x-59.5702x^2+19.6495x^3+0.091464x^4, & x\in\left[\frac{9}{10},\frac{19}{20}\right),\\ -7.98062+48.8796x-61.3023x^2+20.3726x^3+0.0307403x^4, & x\in\left[\frac{19}{20},1\right).\end{cases}\tag{71}$$

Example 7 (see [32]). Consider an analytic solution of (1)

$$v(x,t) = (t+1)\cos \pi x x \in [0,1]. \tag{72}$$

The initial and boundary conditions are to be evaluated from (72). The function $g(x,t)$ is to be chosen accordingly.

The proposed methodology is utilized to acquire the numerical results for this problem. Table 3 shows the efficiency of the presented scheme by comparing the errors with those presented in [32, 34]. Figures 7 and 8 illustrate the 2D and 3D comparison of the exact to approximate solutions. The graphs are in excellent affirmation. The 2D and 3D error functions for this example are shown in Figure 9. The numerical solution when $h = 0.05$, $t = 1$, and $\Delta t = 0.01$ is given as

$$V(x,1) = \begin{cases} 2 - 0.0163534x - 9.84508x^2 + 0.613676x^3 + 1.95785x^4, & x \in \left[0, \frac{1}{20}\right), \\ 1.99985 - 0.00725949x - 10.0272x^2 + 1.83263x^3 + 1.9096x^4, & x \in \left[\frac{1}{20}, \frac{1}{10}\right), \\ 1.99867 + 0.0280521x - 10.3822x^2 + 3.03508x^3 + 1.81434x^4, & x \in \left[\frac{1}{10}, \frac{3}{20}\right), \\ \vdots & \\ \vdots & \\ 3.50607 - 4.37378x - 9.60907x^2 + 10.2924x^3 - 1.81434x^4, & x \in \left[\frac{17}{20}, \frac{9}{10}\right), \\ 4.29238 - 6.92536x - 6.92831x^2 + 9.47104x^3 - 1.9096x^4, & x \in \left[\frac{9}{10}, \frac{19}{20}\right), \\ 5.2899 - 10.0341x - 3.74307x^2 + 8.44509x^3 - 1.95785x^4, & x \in \left[\frac{19}{20}, 1\right). \end{cases} \tag{73}$$

Example 8 (see [22]). Consider the equation (1) with IC

$$v(x,0) = 2\sin^2 \pi x, \tag{74}$$

and the BCs,

$$v(0,t) = 0, v(1,t) = 0. \tag{75}$$

The exact solution of this problems is

$$v(x,t) = 2\left(t^2 + t + 1\right)\sin^2 \pi x. \tag{76}$$

$g(x,t)$ is to be chosen accordingly. The introduced algorithm is employed to the aforementioned problem to obtain the numerical results. A comparison of computed errors with those of [22, 24] is discussed in Table 4. In Figure 10, a closed contrast between exact and approximate solution is exhibited. 3D profiles of both exact and approximate solutions are compared in Figure 11. Figure 12 displays the 2D and 3D error portrayals between the approximate and exact solutions. The numerical solution when $h = 0.05$, $t = 1$, and $\Delta t = 0.01$ is given as

$$V(x,1) = \begin{cases} -0.0162085x + 58.9241x^2 - 18.0337x^3 - 11.5028x^4, & x \in \left[0, \frac{1}{20}\right), \\ 0.0043058 - 0.274697x + 64.0995x^2 - 52.6488x^3 - 10.3781x^4, & x \in \left[\frac{1}{20}, \frac{1}{10}\right), \\ 0.0337757 - 1.16093x + 73.0047x^2 - 82.7609x^3 - 8.23736x^4, & x \in \left[\frac{1}{10}, \frac{3}{20}\right), \\ \vdots & \\ \vdots & \\ -19.1207 + 136.384x - 224.702x^2 + 115.71x^3 - 8.23736x^4, & x \in \left[\frac{17}{20}, \frac{9}{10}\right), \\ 0.802238 + 71.5344x - 156.115x^2 + 94.1611x^3 - 10.3781x^4, & x \in \left[\frac{9}{10}, \frac{19}{20}\right), \\ 29.3714 - 17.7196x - 64.194x^2 + 64.045x^3 - 11.5028x^4, & x \in \left[\frac{19}{20}, 1\right). \end{cases} \tag{77}$$

6. Conclusion

In this study, a numerical technique based on the extended cubic B-spline collocation method for the numerical solution of a second order PIDE is presented. The standard finite difference approach is used to discretize the temporal derivatives, while extended cubic B-splines are used to approximate the spatial derivatives. The stability and convergence of the proposed technique are established to ensure that errors do not magnify. Moreover, experimental outcomes substantiate the validity of the proposed scheme. The scheme's accuracy is confirmed by comparing the numerical results with those computed by some available numerical schemes.

Data Availability

No data were used to support this study.

Conflicts of Interest

The authors declare that they have no conflicts of interest.

Acknowledgments

The authors extend their appreciation to the Deputyship for Research & Innovation, Ministry of Education in Saudi Arabia, for funding this research work through the project number IF-PSAU-2021/01/18696.

References

[1] V. Lakshmikantham and M. Rama, *Theory of Integro-Differential Equations*, vol. 1, CRC Press, 1995.

[2] H. R. Thiem, "A model for the spatial spread of an epidemic," *Journal of Mathematical Biology*, vol. 4, no. 4, pp. 337–351, 1977.

[3] I. Ali, "Jacobi-spectral method for integro-delay differential equations with weakly singular kernels," *Turkish Journal of Mathematics*, vol. 39, pp. 810–819, 2015.

[4] O. M. Ogunlaran and M. O. Oke, "A numerical approach for solving 1st order integro-differential equations," *American Journal of Computational and Applied Mathematics*, vol. 3, no. 4, pp. 214–219, 2013.

[5] K. Chrysafinos, "Approximations of parabolic integro-differential equations using wavelet-Galerkin compression techniques," *BIT Numerical Mathematics*, vol. 47, no. 3, pp. 487–505, 2007.

[6] Z. Abbas, S. Vahdati, K. A. Atan, and L. Nik, "Legendre multi-wavelets direct method for linear integro-differential equations," *Applied Mathematical Sciences*, vol. 3, no. 14, pp. 693–700, 2009.

[7] A. H. Bhrawy, E. Tohidi, and F. Soleymani, "A new Bernoulli matrix method for solving high-order linear and nonlinear Fredholm integro-differential equations with piecewise intervals," *Applied Mathematics and Computation*, vol. 219, no. 2, pp. 482–497, 2012.

[8] S. H. Behiry and H. Hashish, "Wavelet methods for the numerical solution of Fredholm integro-diferential equations," *International Journal of Applied Mathematics*, vol. 11, no. 1, pp. 27–36, 2003.

[9] C. Chen, V. Thome, and L. Wahlbin, "Finite element approximation of a parabolic integro-differential equation with a weakly singular kernel," *Mathematics of Computation*, vol. 58, no. 198, pp. 587–602, 1992.

[10] F. Fakhar-Izadi and M. Dehghan, "The spectral methods for parabolic Volterra integro-differential equations," *Journal of Computational and Applied Mathematics*, vol. 235, no. 14, pp. 4032–4046, 2011.

[11] I. Sloan and V. Thome, "Time discretization of an Integro-differential equation of parabolic type," *SIAM Journal on Numerical Analysis*, vol. 23, no. 5, pp. 1052–1061, 1986.

[12] C. Lubich, "Discretized fractional calculus," *SIAM Journal on Mathematical Analysis*, vol. 17, no. 3, pp. 704–719, 1986.

[13] Z. Sun and X. Wu, "A fully discrete difference scheme for a diffusion-wave system," *Applied Numerical Mathematics*, vol. 56, no. 2, pp. 193–209, 2006.

[14] Y. Lin and C. Xu, "Finite difference/spectral approximations for the time-fractional diffusion equation," *Journal of Computational Physics*, vol. 225, no. 2, pp. 1533–1552, 2007.

[15] S. Larsson, V. Thome, and L. Wahlbin, "Numerical solution of parabolic integro-differential equations by the discontinuous Galerkin method," *Mathematics of Computation*, vol. 67, no. 221, pp. 45–71, 1998.

[16] W. McLean and V. Thome, "Numerical solution of an evolution equation with a positive-type memory term," *The Journal of the Australian Mathematical Society. Series B. Applied Mathematics*, vol. 35, no. 1, pp. 23–70, 1993.

[17] M. A. Ramadan, E. F. Lashien, and W. K. Zahra, "Quintic non-polynomial spline solutions for fourth order two-point boundary value problem," *Communications in Nonlinear Science and Numerical Simulation*, vol. 14, no. 4, pp. 1105–1114, 2009.

[18] M. A. Ramadan, S. F. Talat, and W. K. Zahra, "The use of adomian decomposition method for solving the regularized long-wave equation," *Chaos, Solitons & Fractals*, vol. 26, no. 3, pp. 747–757, 2005.

[19] M. A. Ramadan, E. F. Lashien, and W. K. Zahra, "A class of methods based on a septic non-polynomial spline function for the solution of sixth-order two-point boundary value problems," *International Journal of Computer Mathematics*, vol. 85, no. 5, pp. 759–770, 2008.

[20] T. Tang, "A finite difference scheme for partial integro-differential equations with a weakly singular kernel," *Applied Numerical Mathematics*, vol. 11, no. 4, pp. 309–319, 1993.

[21] M. Dehghan, "Solution of a partial integro-differential equation arising from visco-elasticity," *International Journal of Computer Mathematics*, vol. 83, no. 1, pp. 123–129, 2006.

[22] M. Zarebnia, "Sinc numerical solution for the Volterra integro-differential equation," *Communications in Nonlinear Science and Numerical Simulation*, vol. 15, no. 3, pp. 700–706, 2010.

[23] W. T. Long, D. Xu, and X. Y. Zeng, "Quasi wavelet based numerical method for a class of partial integro- differential equation," *Applied Mathematics and Computation*, vol. 218, no. 24, pp. 11842–11850, 2012.

[24] X. Yang, D. Xu, and H. Zhang, "Crank-Nicolson/quasi-wavelets method for solving fourth order partial integro- differential equation with a weakly singular kernel," *Journal of Computational Physics*, vol. 234, pp. 317–329, 2013.

[25] I. Aziz and I. Khan, "Numerical solution of partial Integro-differential equations of diffusion type," *Mathematical Problems in Engineering*, vol. 2017, 11 pages, 2017.

[26] A. Fahim, M. Araghi, J. Rashidinia, and M. Jalalvand, "Numerical solution of Volterra partial integro-differential equations based on sinc-collocation method," *Advances in Difference Equations*, vol. 2017, no. 1, Article ID 362, 2017.

[27] F. Fakhar-Izadi and M. Dehghan, "An efficient pseudo-spectral Legendre-Galerkin method for solving a nonlinear partial integro-differential equation arising in population dynamics," *Mathematicsl Methods in the Applied Sciences*, vol. 36, no. 12, pp. 1485–1511, 2013.

[28] F. M. Amir and K. Shakibi, "Solving integro-differential equation by using b-spline interpolation," *International Journal of Mathematical Modelling & Computations*, vol. 3, no. 3, pp. 237–244, 2013.

[29] F. Mirzaee and S. Alipour, "Cubic B-spline approximation for linear stochastic integro-differential equation of fractional order," *Journal of Computational and Applied Mathematics*, vol. 366, no. 3, article 112440, 2020.

[30] T. Tahernezhad and R. Jalilian, "Exponential spline for the numerical solutions of Linear Fredholm integro-differential equations," *Advances in Difference Equations*, vol. 2020, no. 1, Article ID 141, 2020.

[31] G. Fairweather, "Spline collocation methods for a class of hyperbolic partial integro-differential equations," *SIAM Journal on Numerical Analysis*, vol. 31, no. 2, pp. 444–460, 1994.

[32] M. Gholamian and J. Saberi-Nadjafi, "Cubic B-splines collocation method for a class of partial integro-differential equation," *Alexandria Engineering Journal*, vol. 57, no. 3, pp. 2157–2165, 2018.

[33] A. Ali, S. Ahmad, S. I. Shah, and F. Haq, "A quartic B-spline collocation technique for the solution of partial integro-differential equations equations with a weakly kernel," *Science International*, vol. 27, no. 4, pp. 2953–2958, 2015.

[34] A. Ali, K. Khan, F. Haq, and S. I. Shah, "A computational modeling based on trigonometric cubic B-spline functions for the approximate solution of a second order partial integro-differential equation," in *Advances in Intelligent Systems and Computing*, Á. Rocha, H. Adeli, L. Reis, and S. Costanzo, Eds., vol. 930 of New Knowledge in Information Systems and Technologies. WorldCIST'19 2019, , pp. 844–854, Springer, 2019.

[35] T. Akram, M. Abbas, A. I. Ismail, N. H. M. Ali, and D. Baleanu, "Extended cubic B-splines in the numerical solution of tme fractional telegraph equation," *Advances in Difference Equations*, vol. 2019, no. 1, 2019.

[36] J. Stoer and R. Bulirsch, *Introduction to Numerical Analysis*, Springer-Verlag, New York, 2nd edition, 1991.

[37] C. de Boor, "On the convergence of odd-degree spline interpolation," *Journal of Approximation Theory*, vol. 1, no. 4, pp. 452–463, 1968.

[38] C. A. Hall, "On error bounds for spline interpolation," *Journal of Approximation Theory*, vol. 1, no. 2, pp. 209–218, 1968.

[39] P. M. Prenter, *Spline and Variational Methods*, Wiley, New-York, 1975.